JOURNAL OF MATERIALS SCIENCE 39 (2004) 2387–2394

Thermal stability of Ti-V-Cr burn-resistant alloys

K. Y. ZHU, Y. Q. ZHAO, H. L. QU, H. WU
Northwest Institute for Nonferrous Metal Research, 710016, Xi'an, People's Republic of China
E-mail: zhu@utt.fr

Ti-35V-15Cr, Ti-25V-15Cr and Ti-25V-15Cr-0.4Si alloys were exposed to different temperatures in air (450–600°C) for aging times between 0 and 200 h and subsequently tensile tested at room temperature with the surface oxide retained or removed. The influence of an applied tensile stress (50–200 MPa) during thermal exposure was also investigated. The results showed that post-exposure tensile properties deteriorated with the increase in exposure temperature and time. The decrease in tensile properties resulted from the combination of surface oxidation and microstructural changes. The main change of the microstructure during thermal exposure is the heterogeneous precipitation of α phase on beta grain boundaries. Both increased vanadium content in the alloy and the addition of silicon have shown an adverse effect on alloys' thermal stability.

1. Introduction

In order to resolve the problem of "titanium fire" which may occur in aeroengines under operating conditions, and meet the requirement for high-performance aerospace materials, "burn resistant" titanium alloys have been studied during the recent years. Several compositions of Ti-V-Cr burn-resistant alloys have been developed in different countries: Ti-35V-15Cr (wt%), designated as Alloy C, was developed by Pratt and Whitney in USA [1]; Ti-25V-15Cr-xAl (wt%) was developed by IRC in UK [2] and Ti-25V-15Cr-xSi (wt%) by NIN in China [3]. There have been some publications on their processability [4], burn-resistant mechanisms [5–8], oxidation behavior [9] and microstructure-properties relationships [10].

Ti-35V-15Cr and Ti-25V-15Cr, whose equivalent molybdenum contents are 47 and 42 respectively [11], are fully β stabilized titanium alloys. β-Ti alloys are attractive in terms of their ability to achieve high strength and they are cold formable in most cases. However, they have been found only limited applications in airframe components and in corrosive environments. The thermal stability of burn-resistant alloys is an essential property since they are new-type β titanium alloys designed to be used under high temperature service conditions. Comprehensive research work on thermal stability has been done on α, near-α, and $\alpha + \beta$ type high temperature titanium alloys, but few investigations have been performed on β titanium alloys. This paper deals with the ability of Ti-25V-15Cr, Ti-35V-15Cr and Ti-25V-15Cr-0.4Si alloys to maintain a stable microstructure and a high level of mechanical properties after exposure to different combinations of time, temperature and tensile stress. The aims are to provide some indepth knowledge of their mechanical behavior and to evaluate the potential application temperatures of these alloys.

2. Experimental procedure

The materials used were alloy bars of Ti-35V-15Cr (alloy A) and Ti-25V-15Cr (alloy B) 11.5 mm in diameter and a pancake of Ti-25V-15Cr-0.4Si (alloy C) 20 mm in thickness. They were manufactured by the Northwest Institute for Nonferrous Metal Research. Their chemical compositions are listed in Table I. After heat treatment, one part of the materials was machined into 5 mm diameter standard tensile specimens with a gauge length of 25 mm. The specimens were machined by turning and then mechanically polished to produce a surface roughness of Ra = 0.1. The tensile specimens were divided into three groups: the ones of the first group were exposed in air at 450, 500, 540 and 600°C for 100 h, the specimens of the second group were exposed at 540°C for 50 and 200 h and the specimens of the third group were exposed in air at 540°C for 100 h with an applied tensile stress of 50, 100 and 200 MPa respectively. During the aforementioned exposures, surface oxide formed on the specimens depending on the temperature and time. The other part of the materials was exposed at 600°C for 100 h and 540°C for 200 h and then machined into 5 mm diameter tensile specimens in order to remove the oxide layer formed during thermal exposures. Finally, the ambient tensile properties of all the specimens were determined comparing the ones with oxide retained and those with oxide removed. Tensile tests were carried out on an Instron testing machine at a speed of 10^{-3} s^{-1}. Three tests at least were performed for each condition. A Philips S-2700 SEM was employed for imaging and a DX-4 spectrometer was used for EDX analysis. TEM specimens were prepared by twin jet polishing using a solution consisting of 95% methanol and 5% $HClO_4$. TEM was carried out on a JEM-200CX transmission electron microscope.

TABLE I Chemical composition of the three alloys (wt%)

Alloy	V	Cr	Si	O	H
A	34.0	13.4	<0.04	0.07	0.001
B	22.9	15.1	<0.04	0.12	0.005
C	24.5	13.6	0.35	0.07	0.001

TABLE II Room temperature tensile properties of the three alloys after thermal exposure at different temperatures

Alloys	Exposure conditions	UTS (MPa)	Y.S. (MPa)	El (%)	R.A. (%)
A	*unexposed*	*1018*	*972*	*7.9*	*12*
	450°C/100 h (1)	983	973	0.8	0.8
	500°C/100 h (1)	963	930	0.8	0.8
	540°C/100 h (1)	945	940	0.4	0.4
	600°C/100 h (1)	816	–	–	– (3)
	600°C/100 h (2)	1015	966	2.8	5.9
B	*unexposed*	*944*	*922*	*18*	*38*
	450°C/100 h (1)	936	895	5.0	6.5
	500°C/100 h (1)	947	910	2.0	4.5
	540°C/100 h (1)	938	925	1.5	4.3
	600°C/100 h (1)	888	–	–	– (3)
	600°C/100 h (2)	974	939	19	45
C	*unexposed*	*959*	*933*	*14*	*19*
	600°C/100 h (1)	–	–	–	– (4)

Note. (1) surface oxide retained; (2) surface oxide removed; (3) El and R.A. could not be accurately measured after post failure due to the peeling of the thick surface oxide; (4) failed into three pieces.

3. Results and discussions

3.1. Tensile test results

After being exposed under different conditions, ambient tensile properties of all specimens were determined and results are listed in Tables II–IV. The reported values represent the average of three valid tests. A test is considered as valid when the failure occurs within the gauge length. It was noted a good reproducibility of yield strength and ultimate tensile strength. The scatter of the elongation to rupture and the reduction in area is around 20%. It can be seen that after thermal exposure, the three alloys exhibit a small reduction in strength and an obvious drop in ductility, especially alloys A and C. The strength and ductility of the three alloys decrease gradually with increased exposure temperature. Comparing the results of alloys A and B with surface oxide retained or removed when they were exposed at 600°C for 100 h (Table II), it has been found that surface oxidation at 600°C is partly responsible for the strength degradation of alloy A whereas the decrease in properties of alloy B after being exposed under similar conditions arise completely from surface oxidation.

TABLE III Room temperature tensile properties of alloys A and B after thermal exposure at 540°C for different times

Alloys	Exposure conditions	UTS (MPa)	Y.S. (MPa)	El (%)	R.A. (%)
A	*unexposed*	*1018*	*972*	*7.9*	*12*
	540°C/50 h (1)	956	950	0.8	0.8
	540°C/100 h (1)	945	940	0.4	0.4
	540°C/200 h (1)	917	–	0.4	0.9
	540°C/200 h (2)	983	947	1.6	3.8
B	*unexposed*	*944*	*922*	*18*	*38*
	540°C/50 h (1)	944	924	6.2	8.0
	540°C/100 h (1)	938	925	1.5	4.3
	540°C/200 h (1)	927	918	1.0	3.9
	540°C/200 h (2)	947	910	3.0	7.4

Note. (1) surface oxide retained; (2) surface oxide removed.

TABLE IV Room temperature tensile properties of alloys A and B after thermal exposure at 540°C for 100 h under different applied stresses

Alloys	Exposure conditions	UTS (MPa)	Y.S. (MPa)	El (%)	R.A. (%)
A	*540°C/100 h (1)*	*945*	*940*	*0.4*	*0.4*
	540°C/50 MPa/100 h (1)	930	904	1.4	2.6
	540°C/100 MPa/100 h (1)	933	908	1.2	4.3
	540°C/200 MPa/100 h (1)	938	903	1.2	3.2
B	*540°C/100 h (1)*	*938*	*925*	*1.5*	*4.3*
	540°C/50 MPa/100 h (1)	866	860	–	– (2)
	540°C/100 MPa/100 h (1)	893	867	3.4	6.7
	540°C/200 MPa/100 h (1)	906	877	2.0	12

Note. (1) surface oxide retained; (2) failed into three pieces.

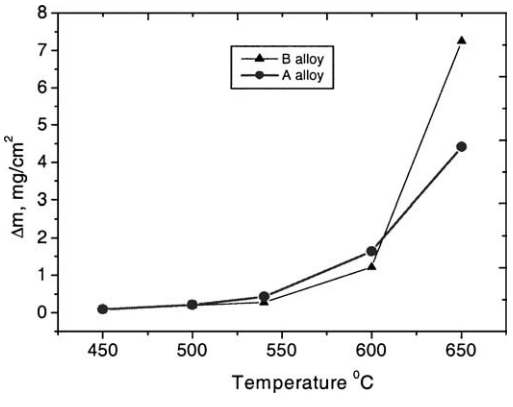

Figure 1 Mass gains of alloys A and B exposed to air at different temperatures for 100 h [13].

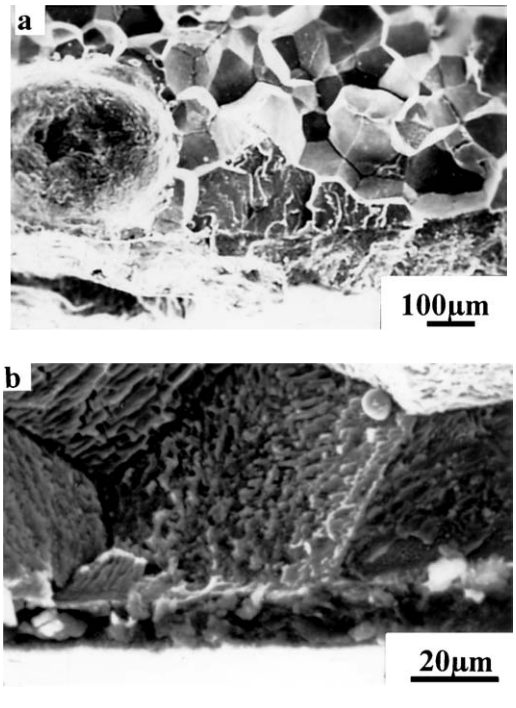

Figure 2 SEM fractographic examination close to surface: (a) alloy A exposed at 600°C for 100 h and (b) alloy B exposed at 540°C for 200 h.

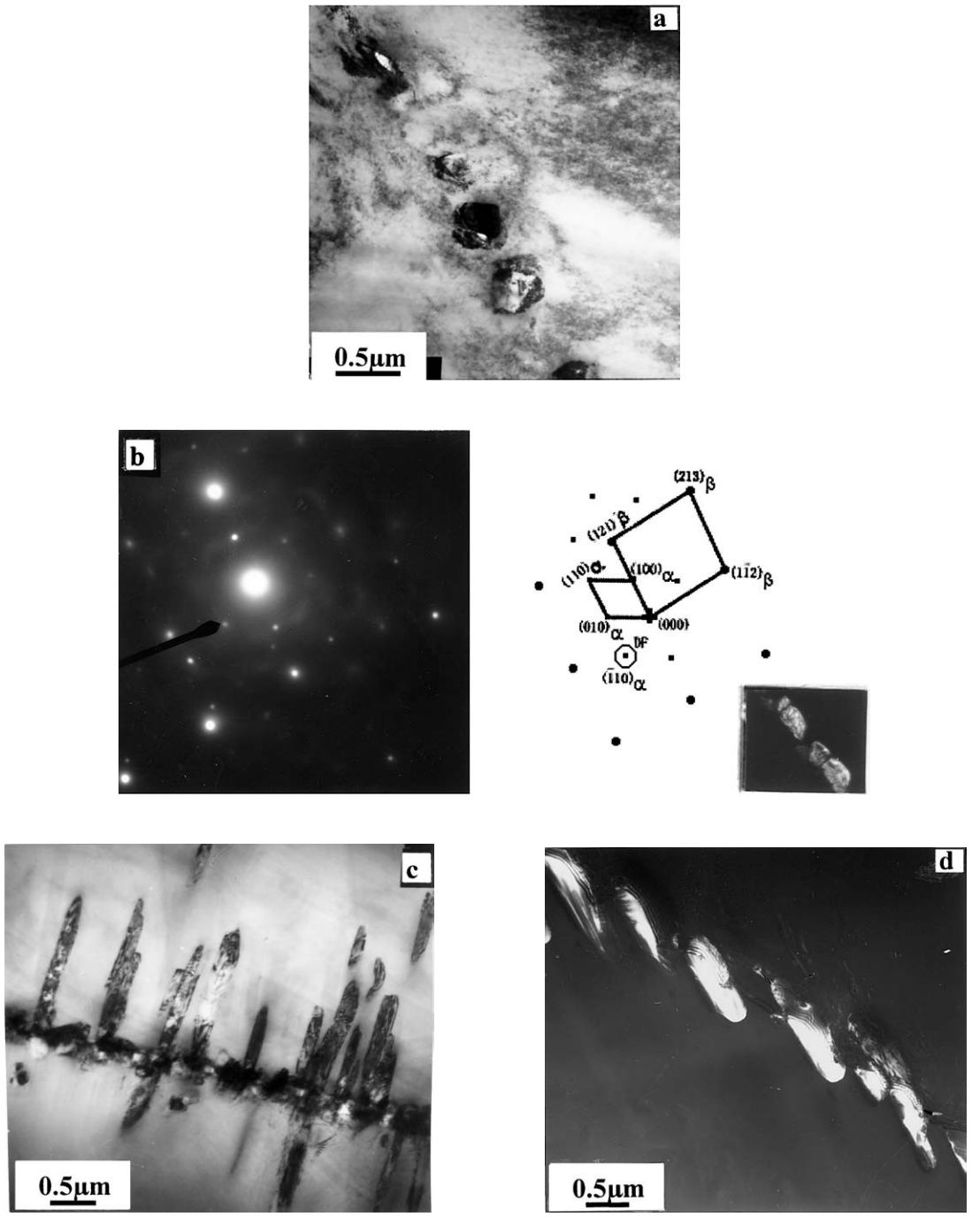

Figure 3 TEM examinations of alloys A and B: (a) grain boundary α phase on unexposed alloy B, (b) ED pattern and identification of α precipitates on grain boundary in alloy B, (c) parallel α laths growing from grain boundary when alloy B exposed at 450°C for 100 h and (d) discontinuous grain boundary α phase in alloy A exposed at 600°C for 100 h.

When the exposure time at 540°C was prolonged (Table III), post-exposure properties of alloys A and B decreased greatly. The comparison of results of alloys A and B exposed at 540°C for 200 h with surface oxide retained or removed, reveals that surface oxide contributes to the reduction of alloys properties. Considering tensile properties after exposure, it can be seen that alloy B displays a better thermal stability than alloy A.

With regard to the effect of an applied tensile stress (Table IV), it was shown that a variation in the range 50–200 MPa has not a significant influence on post-exposure properties of alloys A and B.

3.2. Effect of surface oxidation on thermal stability

Oxidation at temperatures higher than 500°C is one of the main factors that cause the deterioration of titanium alloys. Since the thermally grown oxide is more brittle than the substrate, it is always the origin of cracking. When a titanium alloy is oxidized in air at high temperature, not only does a surface oxidation layer form but also an oxygen diffusion layer develops between the oxide and the alloy substrate. The depth of the crack formed is at least equal to the thickness of oxide and oxygen diffusion layer [12]. The thickness of oxide and

oxygen diffusion layer depends on the exposure temperature and time and the chemical composition of the alloy substrate.

When exposed at different temperatures from 450 to 600°C for 100 h, alloys A and B experienced different degrees of oxidation on their surfaces (Fig. 1). When exposed at a temperature lower than 550°C, alloys A and B exhibit little mass gain, indicating that their mechanical properties may not be significantly affected by oxidation. However, oxidation rates increased quickly as the temperature increased above 550°C. At 600°C, a thick oxide was observed spalling off the surface after tensile testing. That oxide layer is responsible for a severe loss of the ductility (Table II). Fractographic analysis reveals that brittle intergranular failure tends to occur in alloys A and B (Fig. 2).

The surface factor R_s is a parameter that is being used to estimate quantitatively the influence of a surface oxide on the mechanical properties of an alloy [14]. It is defined as follows: $R_s = (\Delta\Psi - \Delta\Psi_0)/\Delta\Psi$, where $\Delta\Psi$ is the variation of reduction in area (R.A.) after thermal exposure with surface oxide and $\Delta\Psi_0$ is the variation of R.A. after thermal exposure without surface oxide. In the case of an exposure at 540°C for 200 h, it has been calculated that R_s values are 26 and 10% for alloys A and B respectively. This indicates that surface oxidation contributes a small part to the alloys properties deterioration, while the larger part comes from changes in their microstructures during thermal exposure. The R_s parameter reveals that surface oxidation has a greater effect on thermal stability in alloy A than in alloy B. As alloy A possesses a higher V content than alloy B, it is worth noting that the present results are consistent with the deleterious influence of V on the oxidation behavior of titanium alloys.

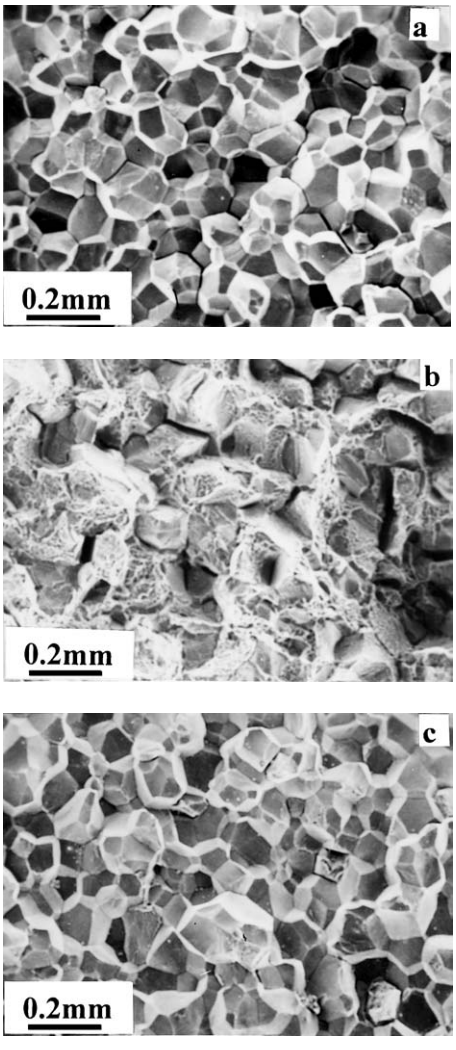

Figure 4 SEM fractographic examinations of alloys A and B exposed at different temperatures: (a) alloy B exposed at 450°C, (b) alloy B exposed at 600°C and (c) alloy A exposed at 600°C.

3.3. Microstructural evolution during thermal exposure

3.3.1. Influence of temperature

It can be observed from the TEM examinations (Fig. 3) that a small amount of discontinuous precipitates exist on the grains boundaries of unexposed alloys A and B (Fig. 3a), while there are few precipitates within the grains. The precipitates were identified to be α phase by electron diffraction (Fig. 3b). When the two alloys were exposed at 450°C for 100 h, the number of α precipitates increased and were distributed heterogeneously. There was also a strong tendency for the α phase to precipitate on β grain boundaries. The α precipitates were mostly plate-shaped and some parallel α laths grew from grain boundaries (Fig. 3c). With increased temperature (450 to 540°C), α precipitates nucleated and grew within grains, while those on grain boundaries became gradually continuous and the parallel α laths growing from grain boundaries coarsened. After exposure at 600°C for 100 h, there was a very small amount of α precipitates in alloys A and B, mainly distributed discontinuously on grain boundaries (Fig. 3d). The dissolution of α phase, especially the grain boundary α phase, would provide great benefit to the ductility of the alloys.

SEM observations (Fig. 4) on fracture surfaces of specimens shows that all thermally exposed specimens fail by brittle intergranular fracture, except for alloy B exposed at 600°C which fails by ductile intergranular fracture. These observations reveal that grain boundary α phase weakens the boundaries and so induces intergranular fracture. Almost all the fracture surfaces of alloy A are smoother than those of alloy B. EDX analysis shows that intergranular facets of alloys A and B are depleted in chromium to 10% and 11 wt% respectively. This is consistent with the lower concentrations of beta alloying elements, such as chromium, which are contained in α phase.

From TEM examinations, it seems that there is a stronger tendency in alloy A than in alloy B for α precipitates to agglomerate on grain boundaries. In order to demonstrate it, polished and then etched cross-sections of the specimens were observed under SEM (Fig. 5). It is shown that there are always lower amounts of α precipitates in alloy A than alloy B, appearing as small white dots in Fig. 5a and b. These observations are in agreement with the phase diagrams of titanium alloys since there are more β stabilizing elements in alloy A than in alloy B. We also could see that grain boundaries of alloys A and B exposed under the same conditions

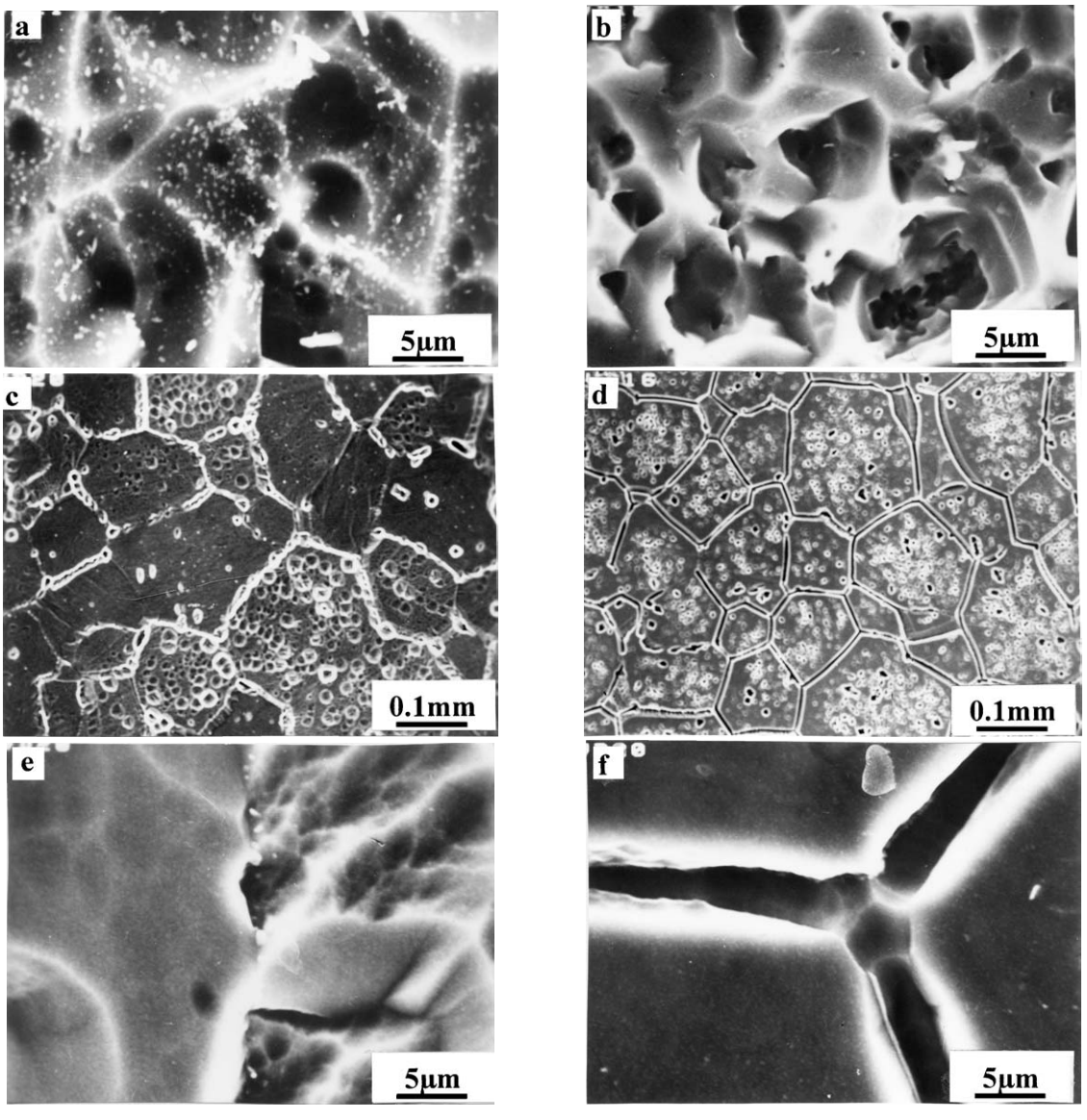

Figure 5 SEM examinations of polished cross-sections: (a) α precipitates within grains in alloy B exposed at 540°C for 100 h, (b) very few α precipitates within grains in alloy A exposed at 540°C for 100 h, (c) morphology of alloy B exposed at 600°C for 100 h at low magnification, (d) microstructure of alloy A exposed at 600°C for 100 h at low magnification, (e) grain boundary of alloy B exposed at 600°C for 100 h at high magnification and (f) grain boundary of alloy A exposed at 600°C for 100 h at high magnification.

have a quite different morphology. For example, considering specimens exposed at 600°C, and observed at a low magnification (Fig. 5c–d), we find that all specimens of alloy A had more delineated and straight grain boundaries than those of alloy B. Then at a higher magnification (Fig. 5e–f), continuous α layers are present on grain boundaries of alloy A whereas only sparse α precipitates appear on grain boundaries of alloy B. It can also be observed that the grain boundary α phase is heavily marked. This can be explained by the lower chromium content in that phase inducing a more severe chemical etching. Therefore, it is suggested that there is a greater tendency for α phase to precipitate on grain boundaries in alloy A than in alloy B, especially after thermal exposure, which contributes strongly to the decrease in ductility exhibited on alloy A as compared with alloy B.

With regard to alloy C before exposure, a very small quantity of α phase and a small amount of Ti_5Si_3 particles (Fig. 6a) exist, which precipitate on grain boundaries and thereby lead to the intergranular fracture of the alloy. When the alloy was exposed at 600°C, α phase is still rarely observed by TEM, but a very large amount of Ti_5Si_3 precipitates are found to be inhomogeneous both in size and distribution, some of them growing in the form of large platelets (Fig. 6b). At the same time, Ti_5Si_3 precipitates on grain boundaries become much denser and bigger. Besides, EDX analysis shows that intergranular fracture facets are poor in Cr (13 wt%) and rich in Si (3 wt%), which suggests the grain boundaries to be Cr-lean and Si-rich.

3.3.2. Influence of time

We can see from TEM observations (Fig. 7) that when alloys A and B were exposed at 540°C, the amount of α precipitates increases gradually and α precipitates distribute heterogeneously with different sizes and shapes with increasing exposure time. Most of the grain boundaries become wider and the α precipitates gather on

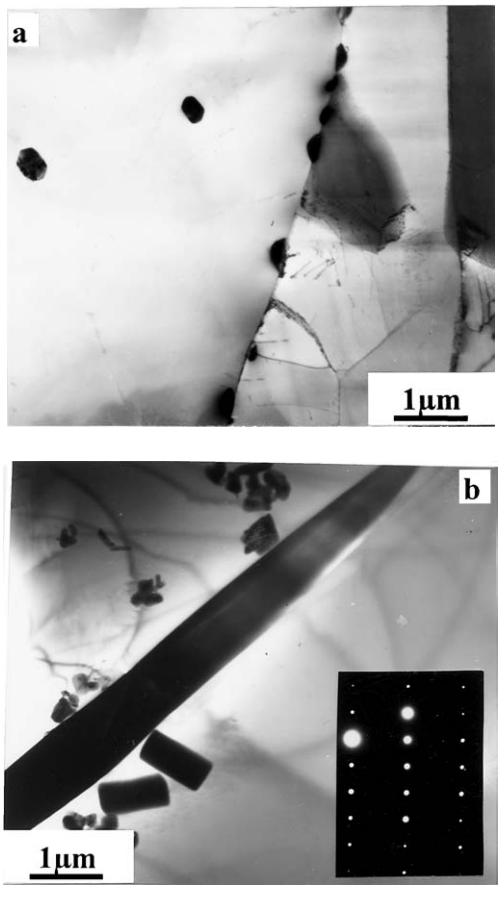

Figure 6 TEM examinations of Ti_5Si_3 precipitates in alloy C: (a) unexposed and (b) exposed at 600°C for 100 h.

grain boundaries, grow and join gradually. At the same time, parallel α laths grow from some grain boundaries and become coarser. From SEM observations on polished and etched cross-sections of specimens exposed at 540°C for different times, it was found that α precipitates in alloy B are always more dense than those in alloy A, but there is a stronger propensity for α precipitates in alloy A to gather on grain boundaries.

When α phase in β titanium alloys is fine and homogeneously dispersed, it has a strengthening effect on the β matrix. In contrast, continuous grain boundary α phase is particularly detrimental to strength, ductility and fracture toughness [16]. SEM observations on the fracture surfaces of the specimens show that all specimens of alloys A and B exposed at 540°C for different times fail by intergranular fracture, which is related to the corresponding low ductility and strength of the grain boundary α phase in the two alloys.

3.3.3. Influence of a tensile stress

SEM and TEM observations (Fig. 8) show that when alloys A and B were exposed at 540°C for 100 h with an applied tensile stress of 50 MPa, stacks of α precipitates distribute heterogeneously in grains with different sizes and shapes such as long acicular, lath and near-oval. It can be seen that dislocations twin around the α phase. In addition, there are a lot of α precipitates on β grain boundaries. When the two alloys were exposed under a 200 MPa tensile stress, the grains contain dense dislocations piles-up that wind around the α precipitates.

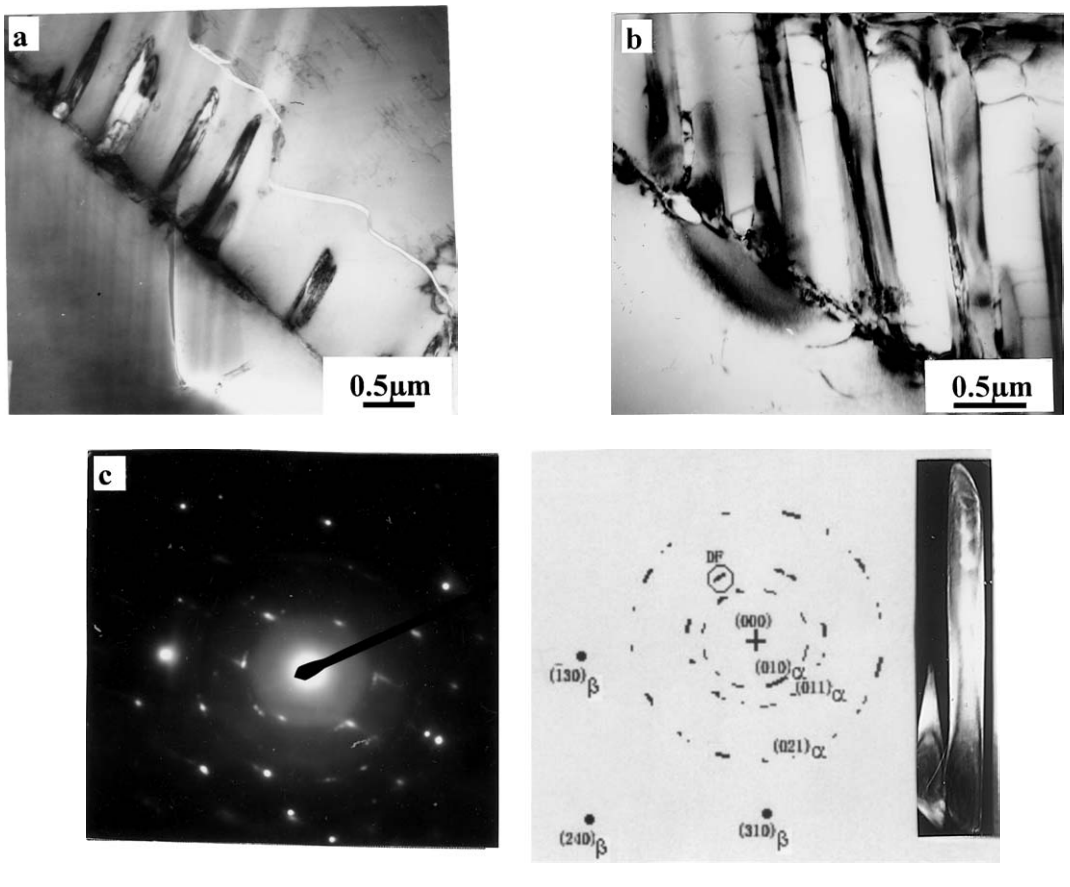

Figure 7 TEM examinations of alloy A exposed at 540°C for different times: (a) 50 h, (b) 200 h and (c) ED pattern and indexation.

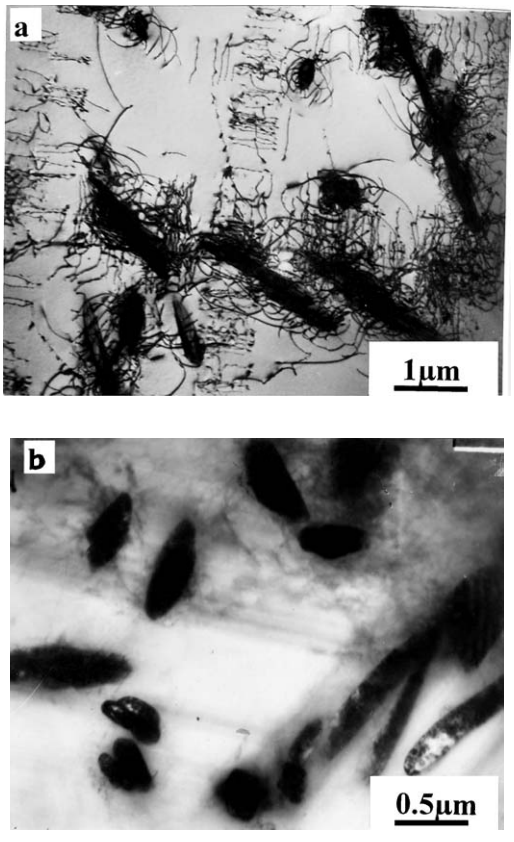

Figure 8 TEM examinations of alloy A exposed under different stresses: (a) 50 MPa and (b) 200 MPa.

Although no obvious change in the amount of α precipitates could easily be observed when the alloys were exposed under different stresses, the size and distribution of α precipitates appear to become much more uniform. Regardless of the exposure stress, α precipitates in alloy B are always more dense than those in alloy A.

According to our SEM and TEM examinations, no evidence exists for a stress-assisted precipitation of the α phase. Also, it has been shown that there is no adverse affect of an applied tensile stress during thermal exposure at 540°C on tensile properties of alloys A and B (Table IV).

3.4. General comments

It can be seen from Ti-Cr binary phase diagram [17] that even a very low Cr content (>0.5 wt%) can lead to the precipitation of $TiCr_2$ phase below the eutectoid temperature (667°C), such as in the case of Ti-5Al-2Cr alloy. Cr exhibits continuous solid solubility with V element which is also a β-isomorphous element, and it has been shown that the addition of V element into Ti-Cr alloys can shrink the $TiCr_2$ phase field and retard the precipitation of $TiCr_2$ [15]. For instance, when the V content in Ti-V-Cr alloy reaches 8 wt%, more than 4 wt% Cr content must be added into the alloy to form the $TiCr_2$ phase at 500°C. This is consistent with our observation of the absence of $TiCr_2$ phase in Ti-25V-15Cr and Ti-35V-15Cr alloys under present experimental conditions. It is also reasonable that ω phase does not appear in the two alloys since they possess a high content of β stabilizing elements and the heat treatment temperatures considered were well above the ω solvus temperature [18].

There is an obvious difference between $\alpha + \beta$ and β-Ti alloys in α-phase nucleation and growth. In $\alpha + \beta$ alloys, the α-phase is either formed by a Widmanstatten type transformation, or by the tempering of martensite. The former often leads to a colony microstructure, which develops rarely in a β-Ti alloy. Moreover, α-phase nucleation tends to be substantially more sluggish in β-Ti alloys. Although this has distinct advantages with regard to hardenability, it makes it difficult to achieve a uniform α-phase distribution. It is therefore very important to identify and control the mode of α-phase nucleation sites for α-phase precipitation in β-Ti alloys. There are five basic types of nucleation sites for α phase precipitation in β-Ti alloys: ω-phase particles, α'' plates, α plates, dislocations and grain boundaries [16]. In the present study, the main nucleation sites for α phase that have been observed during thermal exposure of alloys A and B are grain boundaries. Then, α phase grows either along the grain boundaries or as parallel laths within the grains.

4. Conclusions

1. Under present experimental conditions, post-exposure mechanical properties of alloys A and B deteriorate with the increased temperature and time. An analysis of tensile tests results reveals that surface oxidation contributes to a small part to the degradation of properties of the two alloys whereas the main part arises from the evolution of their microstructures during thermal exposure. It has been found that alloy B exhibits a better thermal stability than alloy A.

2. The main change in the microstructure during thermal exposure of alloys A and B is the heterogeneous precipitation of α phase on beta grain boundaries. Also, parallel α laths grow from some grain boundaries within the grains. There are more α phase precipitates in alloy B than in alloy A owing to the lower content of beta stabilizing elements in alloy B.

3. Precipitation of grain boundary α phase is found to be the main cause for intergranular fracture and tensile properties degradation. The precipitation of α phase on grain boundaries decreases with the increase in the thermal exposure temperature and a concomitant improvement of the ductility has been observed.

4. The addition of Si to alloy B induces the heterogeneous precipitation of Ti_5Si_3 during thermal exposure. This has a deleterious effect on tensile properties.

Acknowledgments

The authors want to show their great gratitude to Dr. A. Vassel (ONERA, France) for his instructive advice on this paper.

References

1. D. M. BERCZIK, U. S. Patent Application, 5176762, 1993.
2. Y. G. LI, P. A. BLENKINSOP, M. H. LORETTO and K. RUGG, *Acta Mater.* **10** (1999) 2889.

3. Y. Q. ZHAO, K. Y. ZHU, H. L. QU and H. WU, *Mater. Sci. Tech*. **16** (2000) 1073.
4. P. A. RUSSO and S. R. SEAGLE, "Titanium '95 Science and Technology," edited by P. A. Blenkinsop, W. J. Evans and H. M. Flower (The Institute of Materials, London, 1996) p. 841.
5. Y. Q. ZHAO, H. L. QU, K. Y. ZHU and H. WU, *Chin. J. Rare Metal Mater. Engin.* **2** (1999) 77.
6. Y. Q. ZHAO, L. ZHOU, K. Y. ZHU, H. L. QU and H. WU, *Chin. J. J. Mater. Sci. Technol*. **6** (2001) 677.
7. Y. Q. ZHAO, H. L. QU, K. Y. ZHU and H. WU, *J. Alloys and Compounds* **284** (1999) 190.
8. Y. Q. ZHAO, K. Y. ZHU, H. L. QU and H. WU, *Mater. Sci. Eng.* A **267** (1999) 167.
9. Y. Q. ZHAO, H. L. QU, K. Y. ZHU and H. WU, *Mater. Sci. Eng*. A **316** (2001) 211.
10. Y. Q. ZHAO, K. Y. ZHU, H. L. QU and H. WU, *ibid.* **282** (2000) 153.
11. D. EYLON, in Proceedings of the International Symposium on Metallurgy and Technology of Practical Titanium Alloys, edited by S. Fujishiro, D. Eylon and T. Kishi (Tokyo, Japan, 1994) p. 29.
12. C. E. SHAMBLEN, in "The Science, Technology and Application of Titanium," edited by R. I. Jaffee and N. E. Promisel (Pergamon Press, UK, 1970) p. 199.
13. H. WU, Y. Q. ZHAO, H. L. QU and K. Y. ZHU, *Chin. J. Rare Metal Mater. and Engin.*, **1** (2003) 45.
14. J. Y. WANG, Z. M. GE and Y. B. ZHOU, "Titanium Alloys on Aeroplanes" (Shanghai Science and Technology Press, 1985) p. 232.
15. B. C. ZHANG, *Chin. J. Rare Metal Mater. Engin.* **4** (1985) 63.
16. T. W. DUERIG and J. C. WILLIAMS, in "Beta Titanium Alloys in the 1980's," edited by R. R. Boyer and H. W. Rosenberg (AIME, Warrendale, USA, 1984) p. 19.
17. "Phase Diagrams of Binary Titanium Alloys," edited by J. L. Murray (ASM, Metals Park, USA, 1987) p. 71.
18. A. VASSEL, in "Beta Titanium Alloys in the 1990's," edited by D. Eylon, R. R. Boyer and D. A. Koss (TMS, Warrendale, USA, 1993) p. 173.

Received 7 May
and accepted 28 October 2003